

Study of ^{168}Dy mass by heavy ion transfer reactions*

Xiuqin Lu, Jiyu Guo, Kui Zhao, Yehao Cheng, Yong Ma, Zhichang Li, Shuyuan Li, Ming Ruan

China Institute of Atomic Energy, P. O. Box 275 (10), Beijing, 102413, People's Republic of China

Received: 23 September 1997 / Revised version: 1 December 1997

Communicated by D. Schwalm

Abstract. The mass of ^{168}Dy has been measured for the first time using the two-proton pick-up reaction $^{170}\text{Er}(^{18}\text{O}, ^{20}\text{Ne})$ at an ^{18}O energy of 104 MeV. The products of the reaction were detected at the focal plane of the Q3D spectrometer. The Q value of the $^{170}\text{Er}(^{18}\text{O}, ^{20}\text{Ne})$ ^{168}Dy reaction was found to be 4.71 ± 0.14 MeV. The mass excess of ^{168}Dy was deduced to be -58.57 ± 0.14 MeV.

PACS. 25.70.Hi Transfer reactions – 27.70.+g $150 \leq A \leq 189$

1 Introduction

The determination of masses of neutron-rich nuclei often presents the first test of the shell model far from the valley of stability, where great differences between experimental results and theoretical predictions as well as among the various theories exist. It also constitutes quantitative information relating to the structure of the nuclei. Quasi-elastic heavy-ion transfer reactions have been extensively used for mass measurements [1–4]. In the present work the reaction of $^{170}\text{Er}(^{18}\text{O}, ^{20}\text{Ne})$ ^{168}Dy has been used in the measurement of the mass of ^{168}Dy , and the experimental mass value of ^{168}Dy is given for the first time.

2 Experimental procedure

The $^{18}\text{O}^{8+}$ beam of 104.0 MeV provided by HI-13 tandem accelerator of CIAE, Beijing, bombarded enriched $^{170}\text{Er}_2\text{O}_3$ target of thickness $280 \mu\text{g}/\text{cm}^2$ on carbon backing of $80 \mu\text{g}/\text{cm}^2$. An enriched $^{164}\text{Er}_2\text{O}_3$ target of thickness $284 \mu\text{g}/\text{cm}^2$ on carbon backing of $100 \mu\text{g}/\text{cm}^2$ was used for calibrations. The enrichment of ^{170}Er and ^{164}Er were 97.7% and 98.0% respectively. The targets were prepared by heavy ion sputtering method. Their thickness were measured with α particle thickness gauging. The reaction products were analyzed by the Beijing Q3D magnetic spectrometer (G120L) and detected by a following gas filled detector [5, 6], which consists of a ΔE -E ionization chamber and two position sensitive counters. The ΔE -E ionization chamber supplies charge identification, while the first position sensitive wire located along the focal plane of the spectrometer supplies position and energy information which was used for mass identification.

The second position wire located 141 mm behind the focal plane together with the first one gives information of the entry angle which enables us to improve the resolution of all energy signals. The entrance aperture of the spectrometer spanned 3° in the reaction plane and subtended a solid angle of 5 msr in present experiment. The Q3D spectrometer positioned at a laboratory angle of 49° , at which the maximum of the cross section was obtained in a prior measurement of the angular distribution of the $^{164}\text{Er}(^{18}\text{O}, ^{20}\text{Ne})$ ^{162}Dy reaction by using a thicker target of $440 \mu\text{g}/\text{cm}^2$. A Au-Si surface barrier detector was fixed at $\theta_1 = 16.5^\circ$ as a monitor in the measurement. The data were recorded by a VAX11/780 computer on-line data acquisition system for off-line analysis. Two dimensional plots of ΔE versus total energy E_t and energy versus focal plane position for all ejected particles and neon ions in the $^{18}\text{O}+^{170}\text{Er}$ reaction at $E_{\text{in}} = 104.0$ MeV and $\theta_1 = 49^\circ$ are presented in Fig. 1 and Fig. 2 respectively. The spectra have been corrected by using the information of the position at focal plane and the entry angles. An unambiguous identification of various ion species was obtained. The neon isotopes were also separated clearly in Fig. 2. Similar plots were obtained for the $^{18}\text{O}+^{164}\text{Er}$ reaction. The ^{20}Ne group from the ^{170}Er target corresponding to the formation of the residual nucleus of ^{168}Dy was gated and the one-dimensional position spectrum was used for determination of the Q-value of the $^{170}\text{Er}(^{18}\text{O}, ^{20}\text{Ne})$ ^{168}Dy reaction.

3 Results and discussion

The focal-plane position spectra of the $^{164}\text{Er}(^{18}\text{O}, ^{20}\text{Ne})$ and $^{170}\text{Er}(^{18}\text{O}, ^{20}\text{Ne})$ reactions with the same Q3D magnetic field setting are shown in Fig. 3. The three strong peaks in the $^{164}\text{Er}(^{18}\text{O}, ^{20}\text{Ne})$ reaction correspond to the ground state, the first and the second excitation states of

* The project supported by the National Natural Science Foundation and the Nuclear Science Foundation of China

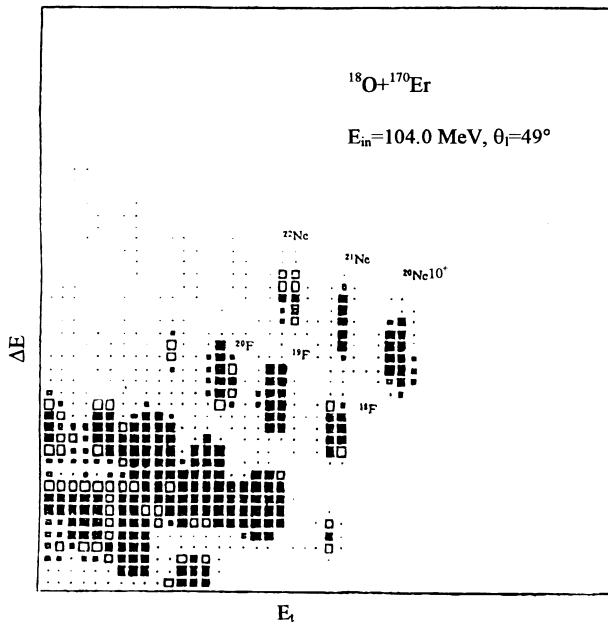


Fig. 1. A portion of a two-dimensional plot of the energy loss ΔE versus the total energy E_t for reaction products from the $^{18}\text{O}+^{170}\text{Er}$ reaction at $E_{in} = 104.0$ MeV, $\vartheta_i = 49^\circ$

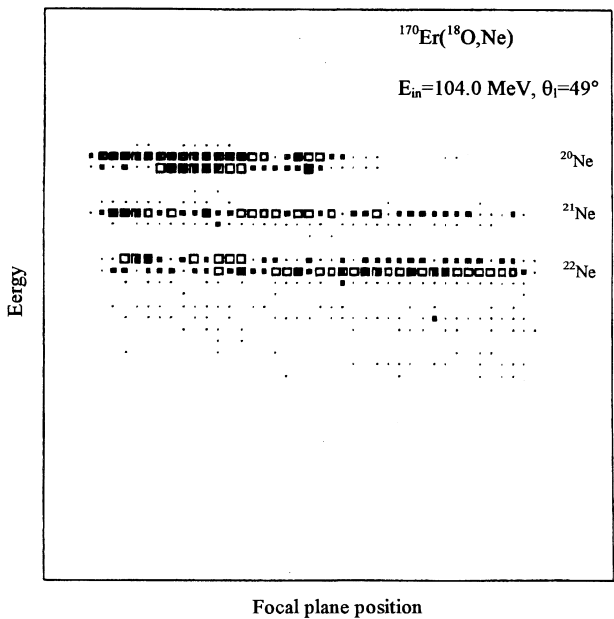


Fig. 2. Two-dimensional plot of the energy versus focal plane position for Ne ions in the $^{18}\text{O}+^{170}\text{Er}$ reaction at $E_{in} = 104.0$ MeV, $\vartheta_i = 49^\circ$

^{20}Ne (1.634 MeV and 4.247 MeV respectively) remaining the residual nucleus ^{162}Dy at its ground state. The two peaks in the $^{170}\text{Er}(^{18}\text{O}, ^{20}\text{Ne})$ reaction correspond to the first two states of ^{20}Ne , while the third one moved out of the detector from the high rigidity end. The energy resolution for ^{20}Ne was 300 keV (fwhm). The Q-value of the $^{170}\text{Er}(^{18}\text{O}, ^{20}\text{Ne})$ reaction was based on the position of the centroid of the ^{20}Ne ground state group relative to

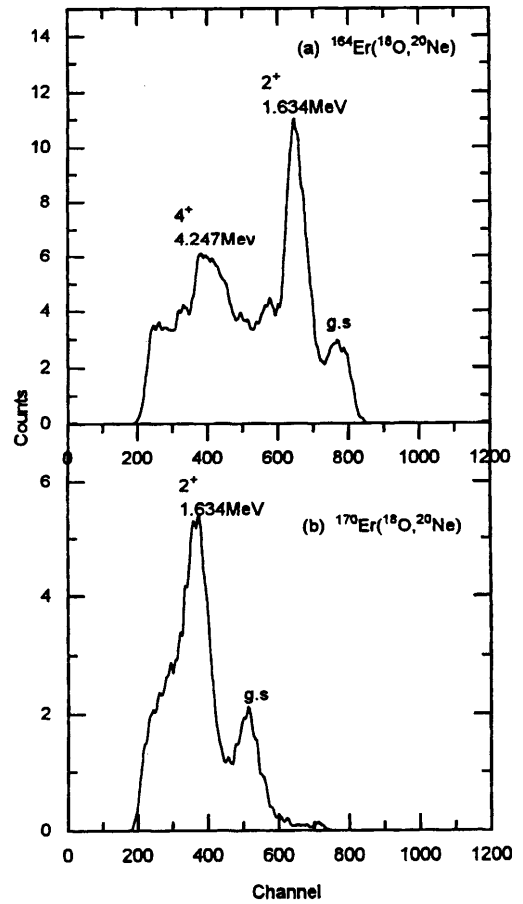


Fig. 3. The focal-plane position spectra of $(^{18}\text{O}, ^{20}\text{Ne})$ on (a) ^{164}Er and (b) ^{170}Er targets respectively at $E_{in} = 104.0$ MeV, $\vartheta_i = 49^\circ$

that from the $^{164}\text{Er}(^{18}\text{O}, ^{20}\text{Ne})$ reaction, together with the measured dispersion at the focal plane of the spectrometer. A calibration of the focal plane was carried out using the ^{18}O elastic scattering on both targets of ^{164}Er and ^{170}Er . The $^{18}\text{O}^{7+}$ beam of the same magnetic rigidity as 104.0 MeV $^{18}\text{O}^{8+}$ beam ($E(^{18}\text{O}^{7+}) = 79.18$ MeV) was employed as the first point of the calibration. At this energy the scattered ^{18}O ions from ^{164}Er and ^{170}Er located just in the same region of Q3D field as $^{20}\text{Ne}^{10+}$ ions from the $^{164}\text{Er}(^{18}\text{O}, ^{20}\text{Ne})$ reaction at $\vartheta_i = 49^\circ$, but the ^{18}O peak sits near the low rigidity end of the focal plane. Starting with this energy the incident energy was decreased by a step of 0.5 MeV until 75.18 MeV. The nine peaks of elastically scattered ^{18}O from each target were obtained for the calibration. The energy loss of ^{18}O and ^{20}Ne in the targets were calculated using the range and stopping power tables of Hubert [7], and the energy was corrected. The stopping power in Er targets was obtained by interpolation between that in Ho and Tm using stopping power in units of MeV/(10^{20} atoms/cm 2). The Q-value of the $^{170}\text{Er}(^{18}\text{O}, ^{20}\text{Ne})$ reaction was obtained to be 4.71 ± 0.14 MeV. The unknown mass excess of ^{168}Dy was deduced to be -58.57 ± 0.14 MeV by means of the known masses of

Table 1. Contributions to the estimated error in ^{168}Dy mass

Source of uncertainty	Contribution(keV)
centroid for $^{170}\text{Er}(^{18}\text{O}, ^{20}\text{Ne})$	52
for $^{164}\text{Er}(^{18}\text{O}, ^{20}\text{Ne})$	44
dispersion calibration fit	29
spectrometer angle (0.2°)	9
absolute beam energy (156 keV)	8
energy loss in target of $^{164}\text{Er}^a$	88
in target of $^{170}\text{Er}^a$	78
mass uncertainty of reference nuclei	4
total	140

^a Includes contributions from the estimated errors in the target thickness and the energy loss of ^{20}Ne and ^{18}O ions.

^{170}Er , ^{18}O , ^{20}Ne and the reaction Q-value. This is the first experimental measured value.

The various contributions to the experimental uncertainty are given in Table 1. The main error comes from the uncertainties of the target thickness, which was 8%, so the errors of the energy loss estimation of ^{18}O and ^{20}Ne ions in the targets were large. The uncertainties from the determination of the centroid of ground state peak of ^{20}Ne for both targets were mainly from the inhomogeneous targets, which were caused by the beam irradiation. When collecting the spectra and calibrating the focal plane the Q3D spectrometer was operated with identical magnetic spectrograph setting, so possible hysteresis was avoided. The started energy of ^{18}O beam used for focal plane calibration was carefully selected as mentioned above, so uncertainty from the absolute beam energy was smaller than that in [4].

The comparison of the measured ^{168}Dy mass-excess value with the theoretical results of model calculations is shown in Table 2. The results compiled in [8] and the prediction of Möller's more recent reformulation [9] are all included in the table. It can be seen that the value we obtained in error range is in agreement with the predictions of Möller-Nix, Tachibana and Jänecke-Masson. It lies almost midway between Möller's two predictions and differs about 200 keV with others.

The authors wish to thank the staff in the division of Tandem accelerator of CIAE for the efficient running of the machine, and to thank Dr. Xu Guo-ji for his preparing the targets.

Table 2. Comparison of the measured ^{168}Dy mass with the results of various model calculations

Present work	Mass excess (MeV)	
	Ref. 8	Ref. 9
-58.57 ± 0.14	$-58.12^a)$	$-58.90^i)$
	$-58.68^b)$	
	$-59.65 \pm 0.70^c)$	
	$-58.84^d)$	
	$-58.73^e)$	
	$-58.06^f)$	
	$-58.48^g)$	
	$-58.80^h)$	

^{a)} Möller et al., finite-range droplet model and a folded-Yukawa single-particle potential.

^{b)} Möller-Nix, from unified macroscopic-microscopic model.

^{c)} Comay-Kelson-Zidon, predictions by modified ensemble averaging.

^{d)} Satpathy-Nayakin, finite nuclear matter model.

^{e)} Tachibana et al., empirical mass formula with proton-neutron interaction.

^{f)} Spanier-Johannson, Modified Bethe-Weizsäcker mass formula.

^{g)} Jänecke-Masson, Garvey-Kelson mass relations.

^{h)} Masson-Jänecke, inhomogeneous partial difference equation.

ⁱ⁾ Möller et al., a) with improvement.

References

1. P.H. Dessagne, M. Bernas, M. Langevin et al.: Nucl. Phys. **A426**, 399 (1984)
2. P.J. Woods, R. Chapman, J. L. Durell et al.: Z. Phys. **A321**, 119 (1985)
3. W.N. Catford, L.K. Fifield, Orr N A: Nucl. Phys. **A503**, 263 (1989)
4. Kui Zhao, Jiyu Guo, Xiuqin Lu et al.: Z. Phys. **A357**, 75 (1997)
5. Li Zhichang, Cheng Ye-hao, Yan Chen et al.: Nucl. Instr. & Meth. **A336**, 150 (1993)
6. Guo Ji-yu, Zhao Kui, Li Zhi-Chang et al.: Chin. Jour. of Nucl. Phys. **17**, 73 (1995)
7. F. Hubert, R. Bimbot and H. Gauvin : At. Data and Nucl. Data Tables, **46**, 1 (1990)
8. P.E. Haustein : At. Data Nucl. Data Tables **39**, 281 (1988)
9. P. Möller, J.R. Nix, W.D. Myers et al.: At. Data Nucl. Data Tables, **59**, 185 (1995)